Volume : 3 | Issue : 8 | Aug 2014 • ISSN No 2277 - 8179

Research Paper

Preparation and Characterization of Graphene/Poly M-Chloroaniline Conducting Polymer Composites

Physics

KEYWORDS : Graphene oxide; composite, polymer; Poly metachloroaniline;

Ashok Kumar Mishra Department of Physics, Ravenshaw University, Cuttack, Odisha, India.

Gourisankar Roy Department of Physics, Ravenshaw University, Cuttack, Odisha, India.

ABSTRACT

In the present research program, we have described the synthesis of Poly metachloroaniline–graphene (PmClAn/RGO) nanocomposites were prepared via in situ bulk polymerization using two different preparation techniques. In the first approach, a mixture of graphite oxide (GO) and Poly (PmClAn)monomers (PmClAn) were polymerized using a bulk polymerization method with a free radical initiator. After the addition of the reducing agent hydrazine hydrate (HH), the product was reduced via microwave irradiation (MWI) to obtain R-(GO-PmClAn) composites. In the second approach, a mixture of graphite sheets (RGO) and PmClAn monomers were polymerized using a bulk polymerization method with a free radical initiator to obtain RGO-(PmClAn) composites. The composites were characterized by FTIR, XRD, SEM and conductivity. The results indicate that the composite obtained using the first approach, which involved MWI, had a better morphology and dispersion with enhanced thermal stability compared with the composites prepared without MWI.

Introduction:

In last couples of years, graphene has been used as alternative carbon-based nanofiller in the preparation of polymer nanocomposites and have shown improved mechanical, thermal, and electrical properties .The recent advances have shown that it can replace brittle and chemically unstable indium tin oxide in flexible displays and touch screens [1-4] . It is well established that the superior properties of graphene are associated with its single-layer. However, the fabrication of single-layer graphene is difficult at ambient temperature. If the sheets are not well separated from each other than graphene sheets with a high surface area tend to form irreversible agglomerates and restacks to form graphite through p–p stacking and Vander Waals interactions . Aggregation can be reduced by the attachment of other small molecules or polymers to the graphene sheets [5-8].

Graphene consists of a honeycomb lattice of carbon atoms. It is a purely two-dimensional material, were the sp^2-bonds between the carbon atoms [9-11] are responsible for the high mechanical strength of the sheet. The binding between different graphene layers, in multilayer graphene or graphite is much weaker, since it is mostly due to van der Waals interactions. The π conjugate system, constituted by the carbon p_z-orbitals, is responsible for electrical conductivity of the graphene layer. Since it can be seen as the basic building block for other carbon allotropes such as fullerenes [12-15], carbon nanotubes [16], or graphite, its band structure has been intensively studied theoretically [17-19]. Tight binding calculation of graphene's band structure reveals an unusual semimetallic behavior with a linear dispersion around the meeting points of the conduction and valance band. Here, the charge carriers are mass-less and mimic relativistic particles, such as photons. This makes it possible to study quantum electrodynamics in a solid state material [20,21].

One of the advantages of graphene oxide (GO) is that it can be easily dispersed in water and physiological environments due to its abundant hydrophilic groups, which include hydroxyl, epoxide and carboxylic groups on its large surface . Recently, the El-Shall group demonstrated a novel approach for the production of GR sheets (RGO) prepared via the Hoffman Hummers method via reduction of GO using hydrazine hydrate (HH) facilated by using MWI. The resulting product is composed of graphene sheets with polar functional groups, even after the reduction [22]. GO has an affinity for polar solvents and polymers [23]. This affinity makes GO an important intermediate in the preparation of RGO polymer composites via chemical reduction.

A survey of the literature reveals that m-chloroaniline has not been polymerized in the presence of modified graphene. We wish to present here the synthesis and characterization of polymerization m-chloroaniline with functionalized graphene with different ratios of graphene. The composites have been characterized using FTIR, SEM, XRD, and conductivity.

Experimental

Materials

Graphite powder, H2SO4, NaNO3, NaOH, H2O2 (30%), K3Fe (CN)6 and KMnO4 were purchased from Sigma-Aldrich . All the chemicals were of analytical reagent grades and used as received, without further purifications. The aqueous solutions were prepared in Milli-Q water (18 MΩ cm-1).

Preparation of Graphite Oxide (GO)

Graphene oxide (GO) was synthesized from graphite powder using modified Hummer's method. In brief, 1 g of graphite and 0.5 g of sodium nitrate were mixed together followed by the addition of 23 ml of conc. sulphuric acid under constant stirring. After 1 h, 3 g of KMnO4 was added gradually to the above solution while keeping the temperature less than 20°C to prevent overheating and explosion. The mixture was stirred at 35 °C for 12 h and the resulting solution was diluted by adding 500 ml of water under vigorous stirring. To ensure the completion of reaction with KMnO4, the suspension was further treated with 30% H2O2 solution (5 ml). The resulting mixture was washed with HCl and H2O respectively, followed by filtration and drying, graphene oxide sheets were thus obtained.

Preparation of RGO

The dried GO (400 mg) was stirred and sonicated in deionized water (20 mL) until a homogeneous yellow dispersion was obtained. The GO can be dispersed easily in water due to the presence of a variety of hydrophilic oxygen groups (OH, O and COOH) on the basal planes and edges. The solution was placed inside a conventional microwave after the addition of HH reducing agent (400 μL). The microwave oven was operated at full power in 30 s cycles (on for 10 s and off and stirring for 20 s) for a total reaction time of 2 min [16]. The yellow dispersion of GO gradually changed to a black color indicating the completion of the chemical reduction to RGO. The RGO sheets were separated using a centrifuge (Centurion Scientific Ltd., West Sussex, UK) operated at 6,000 rpm for 25 min and dried at 70 °C overnight.

Preparation of the RGO-(PmClAn) Nanocomposites via the in Situ Method

RGO powder [2.0 (wt./wt.%)] was added to the PmClAn

Volume : 3 | Issue : 8 | Aug 2014 • ISSN No 2277 - 8179

monomer, stirred and sonicated for 1 h. The benzoyl peroxide (BP) initiator (5.0 wt.%) was added to the suspension and stirred until the initiator dissolved. Then, the mixture was heated to 60 °C to initiate the polymerization using a shaking-water bath. The reaction mixture was maintained at 60 °C for 20 h. After the polymerization finished, the product was poured into an excess of methanol, stirred for 20 min and washed with hot water to remove the PmClA nmonomers. Then, the product was filtered and dried at 80 °C overnight.

Preparation of the R-(GO-PmClAn) Nanocomposites via the MWI Method

GO powder [2.0 (wt./wt.%)] was added to the PmClAn monomer, stirred and sonicated for 1 h. The benzoyl peroxide (BP) initiator (5.0 wt.%) was added to the suspension and stirred until the initiator dissolved. Then, the reaction mixture was maintained at 60 °C for 20 h to promote polymerization using a shaking-water bath (GFL). After the polymerization finished, the product was poured into an excess of methanol, stirred for 15 min and washed with hot water to remove PmClAn monomers. Then, the product was filtered and dried at 80 °C overnight. Four hundred milligrams of the dried composite of GO-PmClAn was dissolved in DMF, stirred and sonicated for 1 h. Then, the composite was placed inside a conventional microwave oven (Kenwood MW740) following the addition of HH (400 µL). The microwave oven was operated at full power (900 W) in 30 s cycles (on for 10 s and off and stirring for 20 s) for a total reaction time of 2 min [16]. Then, the composites were separated using a centrifuge (Centurion Scientific Ltd.) operated at 5,000 rpm for 15 min and dried in an oven at 70 °C overnight. For comparison, the neat PmClAn was prepared via a similar procedure in the absence of the RGO and GO.

Measurement:

IR spectra:

The Fourier Transform Infrared (FT-IR) spectra were recorded on a Nicolet 8700 spectrometer, in the range 400–4000 cm-1.

XRD:

X-ray diffraction (Rigaku, D/Max, 2500V, Cu-Kα radiation: 1.54056A°) experiments were carried out on both the plain PmClAn and the composite samples. Wide-angle X-ray diffractograms were recorded at temperature of 300 C after isothermal crystallization at this temperature for 1 h in the range of 0-70(2q).

SEM:

Morphology of the PmClAn/c-graphene composite was investigated using a Philip XL 30 scanning electron microscope at an accelerating voltage of 25 kV. The sample was fractured at liquid nitrogen temperature and then was coated with a thin layer of gold before observation.

Conductivity:

The standard Van Der Pauw DC four probe method was used to measure the electron transport behavior of PmClAn, PmClAn/c-graphene composites. The samples of PmClAn and PmClAn/c- graphene were pressed into pellet. The pellet was cut into a square. The square was placed on the four probe apparatus, providing a voltage for the corresponding electrical current could be obtained. The electrical conductivity of samples was calculated by the following formula: σ (S/cm) =(2.44 ×10/*S*) ×(I/E), where σ is the conductivity; *S* is the sample side area; *I* is the current passed through outer probes; *E* is the voltage drop across inner probes.

Result and Discussion:

FTIR spectral analysis:

FTIR spectral analysis was performed to confirm the chemical structure of all of the RGO/ (PmClAn) nanocomposites. Figure 1 summarizes the FTIR spectra of the GO, RGO, neat PmClAn, RGO-(PmClAn) and R-(GO- PmClAn) nanocomposites. In figure 1a, the characteristic FTIR features of GO include the presence of different types of oxygen functionalities, which have been confirmed by the band at 3421 $cm^{-1,}$ which corresponds to the O-H group, the bands at 1722 and 1620 cm−1, which correspond to the C=O carbonyl/carboxyl and C=C aromatic groups, respectively, and the band at 1223 cm−1, which corresponds with the C-O . In figure 1b, indicates that the O-H band at 3431 cm^{-1} was reduced in intensity due to the deoxygenation of the GO-oxygenated functionalities. The spectrum of RGO also contains bands at 1625 cm^{-1} and 1141 $cm^{-1,}$ which correspond to C=C and C-O groups, respectively. The spectrum also had a band at 1151 cm^{-1} that has been assigned to the C-O-C group. The bands between 1272 cm^{-1} and 992 cm^{-1} originate from the C-O group. For the RGO-(PmClAn) nanocomposites, In figure 1c shows the characteristic bands at 3421, 1725 and 1622 cm^{-1} that correspond to the O–H, C=O and C=C groups for the RGO-(PmClAn) nanocomposites, respectively . When MWI was employed in the preparation of R-(GO- PmClAn) nanocomposites (Figure 1d), there was an increase in the intensity of the C=C bands and a decrease in the intensity of the C=O bands. In addition, strong characteristic bands associated with aliphatic C-H and -CH_2 groups were observed at 2921 and 2856 $cm^{-1,}$ respectively, in the spectrum of the R-(GO- PmClAn) nanocomposites .

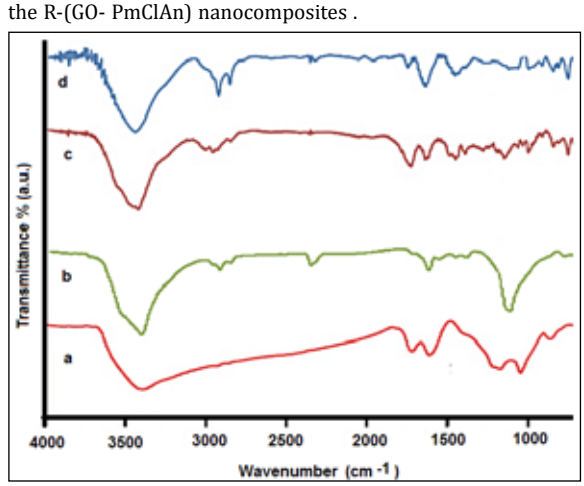

Figure 1.FTIR spectra of (a) GO; (b) RGO; (c) RGO-(PmClA) nanocomposites and (d) R-(GO-PmClA) nanocomposites

XRD

The X-ray diffraction data for RGO, RGO-(PmClAn) and R-(GO- PmClAn) composites are shown in Fig. 2. The XRD pattern of GO displayed in Figure 2a showed a characteristic peak (2θ) at approximately 9.33°, which corresponds with a d-spacing of 0.95 nm. After GO was reduced (Figure 2b), the d-spacing decreased. In addition, the peak appeared at 2θ = 12.41°, with a d-spacing of 0.71 nm. This result confirms the chemical reduction of GO and formation of RGO . In addition, this result also indicates the removal of large number of oxygen-containing groups and the formation of much more exfoliated RGO sheets, as well as a change in the hybridization of the reduced carbon atoms from tetrahedral sp3 to planar sp2 . The XRD pattern of the RGO-(PmClAn) nanocomposites (Figure 2c) had a broad peak, indicating an amorphous structure, which corresponds primarily with the PmClAn with a 2θ of 27.40° and a d-spacing of 0.32 nm. The XRD pattern of the prepared R-(GO- PmClAn) nanocomposites prepared via MWI (Figure 2d) showed an increase in the d-spacing, with a band at 2θ = 26.70° and a d-spacing of 0.33 nm. In addition, the characteristic peaks of RGO and GO do not appear in the patterns of the composites, which indicates that the RGO layers were exfoliated in the composites .

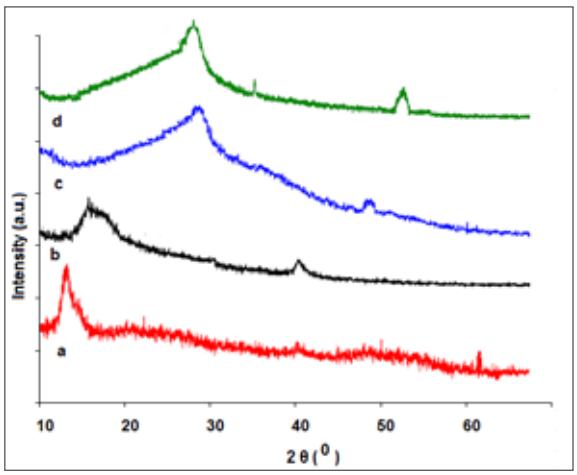

Figure 2.XRD patterns of (a) Graphite; (b) GO; (c) RGO; (d) RGO-(PmClA) nanocomposites and (e) R-(GO-PmClA) nanocomposites

SEM

The SEM pictures of the GO, RGO, RGO-(PmClAn) and R-(GO- PmClAn) composites, in Fig. 3. Figure 3a shows the prepared GO (Figure 3a) was not fully exfoliated and had a flaky texture. This result suggests a partially exfoliated structure and reflects its layered microstructure containing large interlayer spacing and thick multilayer stacks. Figure 3b shows the SEM image of RGO, which reveals that the RGO consisted of randomly aggregated thin crumpled sheets that are closely associated with each other, forming a disordered solid . The SEM image of the RGO-(PMMA) nanocomposites prepared via the *in situ* method (Figure 3c) shows that RGO is stacked up, and not well dispersed in the PmClAn matrix. For the R-(GO- PmClAn) nanocomposites (Figure 3d), the wrinkled and crumpled profile of RGO was observed with significant changes in the morphology .

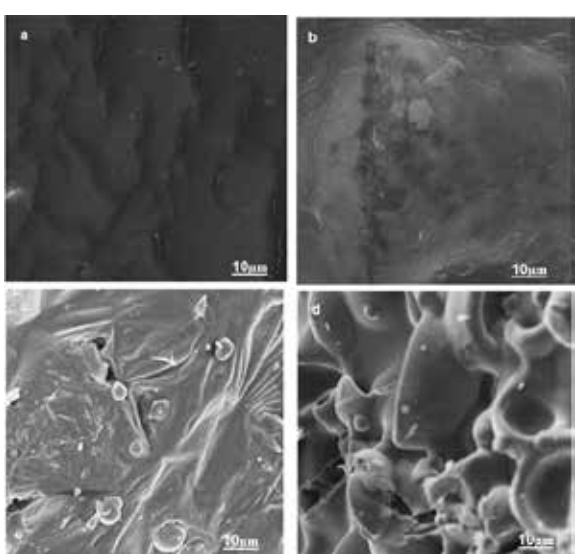

Figure 3.The SEM micrographs of (a) GO; (b) RGO; (c) RGO-(PmClA) nanocomposites; (d) R-(GO-PmClA) nanocomposites

Conductivity:

The electrical conductivities PmClAn/RGO composites were measured using the standard Van Der Pauw DC four-probe method shown in Fig. 4 . The conductivity of PmClAn synthesized in the presence of hydrochloric acid at room temperature is of 1.11× 10-4 S/cm. Meanwhile, by the addition of 2 wt% RGO into PmClAn, the conductivity at room temperature increases from 1.11 to 8×10-4 S/cm. Further, the conductivity at room temperature gradually increases to 11× 10-4, 19 ×10-4 S/cm for 5 and 10 wt% RGO ccontent. The reason for improvement in conductivity is the π–π* interaction between the surface of RGO and the quinoid ring of the copolymer chain .

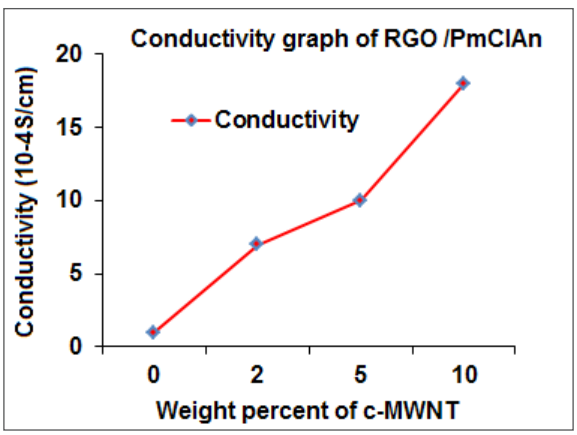

Fig. 4 Conductivity versus the weight percent of RGO /PmClAn composites

Conclusions

R-(GO-PmClAn) and RGO-(PmClAn) using in situ bulk polymerization facilitated by MWI. The nanocomposites were characterized using FT-IR , XRD, SEM and conductivity analysis. The morphology of RGO-(PmClAn) composites contains both the thinner fibrous phase and the larger block phase. It is assumed that RGO-(PmClAn) were used as a core in the formation of tubular shells of the fibrous PmClAn /c-MWNT composites. The highly ordered structures of nanocomposites were confirmed by XRD patterns. Room temperature conductivity of nanocomposite increased with the increase of RGO.

REFERENCE

1. Novoselov, K.S., Geim, A.K.; Morozov, S.V.; Jiang, D.; Zhang, Y., Dubonos, S.V.; Grigorieva, I.V.; Firsov, A.A. Electric field effect in atomically thin carbon films. Science 2004, 306, 666–669. | 2. Stoller, M.D.; Park, S.; Zhu, Y.; An, J.; Ruoff, R.S. Graphene-based ultracapacitors. Nano. Lett. 2008, 8, 3498–3502. | 3. Nair, R.R.; Blake, P.; Grigorenko, A.N.; Novoselov, K.S.; Booth, T.J.; Stauber, T.I.; Peres, N.M.R.; Geim, A.K. Fine structure constant defines visual transparency of graphene. Science 2008, 320, 1308–1308. | 4. Lee, C.; Wei, X.D.; Kysar, J.W.; Hone, J. Measurement of the elastic properties of intrinsic strength of monolayer graphene. Science 2008, 321, 385–388. | 5. Balandin, A.A.; Ghosh, S.; Bao, W.; Calizo, I.; Teweldebrhan, D.; Miao, F.; Lau, C N. Superior thermal conductivity of single-layer graphene. Nano Lett. 2008, 8, 902–907. | 6. Stankovich, S.; Dikin, D.A.; Dommett, G.H.B.; Kohlhaas, K.M.; Zimney, E.J.; Stach, E.A.; et al. Graphene-based composite materials. Nature 2006, 442, 282–286. | 7. Ramanathan, T.; Abdala, A.A.; Stankovich, S.; Dikin, D.A.; Alonso, M.H.; Piner, R.D.; et al. Functionalized graphene sheets for polymer nanocomposites. Nat. Nanotechnol. 2008, 3, 327–331. | 8. Lee, Y.R.; Raghu, A.V.; Jeong, H.M.; Kim, B.K. Properties of waterborne polyurethane=functionalized graphene sheet nanocomposites prepared by an in situ method. Macromol. Chem. Phys. 2009, 210, 1247–1254. | 9. Xu,Y.;Wang,Y.; Jiajie, L.;Huang,Y.;Ma,Y.;Wan,X.; et al.Ahybrid material of graphene and poly (3,4-ethyldioxythiophene) with high conductivity, flexibility, and transparency. Nano Res. 2009, 2, 343–348. | 10. Quan, H.; Zhang, B.; Zhao, Q.; Yuen, R.K.K.; Li, R.K.Y. Facile preparation and thermal degradation studies of graphite nanoplatelets (GNPs) filled thermoplastic p olyurethane (TPU) nanocomposites. Compos. Pt. A 2009, 40, 1506–1513. | 11. Liang, J.; Huang, Y.; Zhang, L.; Wang, Y.; Ma, Y.; Guo, T.; et al. Molecular-level dispersion of graphene into poly(vinyl alcohol) and effective reinforcement of their nanocomposites. Adv. Funct. Mater. 2009, 19, 2297–2302. | 12. Balog, R.; Jørgensen, B.; Nilsson, L.; Andersen, M.; Rienks, E.; Bianchi, M.; et al. Bandgap opening in graphene induced by patterned hydrogen adsorption. Nat. Mater. 2010, 9, 315–319. | 13. Zhao, H.; Min, K.; Aluru, N.R. Size and chirality dependent elastic properties of graphene nanoribbons under uniaxial tension. Nano Lett. 2009, 9, 3012–3015. | 14. Scarpa, F.; Adhikari, S.; Phani, A.S. Effective elastic mechanical properties of single layer graphene sheets. Nanotechnology 2009, 20, 065709=1–11. | 15. Kudin, K.N.; Scuseria, G.E.; Yakobson, B.I. Oxygen-driven unzipping graphite materials. Phys. Rev. B 2001, 64, 235406=1–4. | 16. Hummers Jr, W. S. & Offeman, R. E. Preparation of graphitic oxide. J. Am. Chem. Soc. 80, 1339–1339 (1958). | 17. Park, S. & Ruoff, R. S. Chemical methods for the production of graphenes. Nat. Nanotechnol. 4, 217–224 (2009). | 18. Kim, S. et al. Room-temperature metastability of multilayer graphene oxide films. Nat. Mater. 11, 544–549 (2012). | 19. Li, X. et al.Highly conducting graphene sheets and Langmuir–Blodgett films. Nat. Nanotechnol. 3, 538–542 (2008). | 20. Stankovich, S. et al. Synthesis of graphene-based nanosheets via chemical reduction of exfoliated graphite oxide. Carbon 45, 1558–1565 (2007). | 21. Pei, S., Zhao, J., Du, J., Ren, W. & Cheng, H. Direct reduction of graphene oxide films into highly conductive and flexible graphene films by hydrohalic acids. Carbon 48, 4466–4474 (2010). | 22. El-Shall, M.S.; Abdelsayed, V.; Khder, A.S.; Hassan, H.; El-Kaderi, H.M.; Reich, T.E. Metallic and bimetallic nanocatalysts incorporated into highly porous coordination polymer MIL-101. J. Mater. Chem. 2009, 19, 7625–7631. | 23. Potts, J.R.; Lee, S.H.; Alam, T.M.; An, J.; Stoller, M.D.; Piner, R.D.; Ruoff, R.S.Thermomechanical properties of chemically modified graphene/poly(methyl methacrylate) composites made by in situ polymerization. Carbon 2011, 49, 2615–2623 |